Available online at www.sciencedirect.com

ScienceDirect

Procedia Structural Integrity 24 (2019) 775–787

Structural Integrity Procedia

www.elsevier.com/locate/procedia

AIAS 2019 International Conference on Stress Analysis

CAE^{Up} - Update of CAE models on actual manufactured shapes

Stefano Porziani[a], Francesco Scarpitta[a], Emiliano Costa[b], Edoardo Ferrante[b], Biagio Capacchione[c], Michel Rochette[d], Marco Evangelos Biancolini[a,*]

[a] *University of Rome "Tor Vergata", Via Politecnico 1, Rome 00133, Italy*
[b] *RINA Consulting S.p.A.,Viale Cesare Pavese, 305, Rome 00144, Italy*
[c] *CMS Spa, Via Nuova Strada Consortile - 84084 Fisciano (SA), Italy*
[d] *ANSYS France, 11 Avenue Albert Einstein, 69100 Villeurbanne, France*

Abstract

Engineering fields with high technological contents involve manufacturing requirements in which the control of the margins of tolerance, as well as the verification of the manufactured components, has economic impacts in the relationships with customers. The verification of the actual geometry after manufacturing then acquires paramount importance, and it can be substantially improved by adopting the digital twin approach: the CAE model of the system is adapted onto the actual manufactured shape making the numerical prediction individual manufactured component specific. CAE^{Up} aims at implementing a cloud-based software tool whose core is the comparison of the structural performances between the CAE model relative to the nominal design of a certain product and the digital twin of the real product as built. The digital twin is updated on High Performance Computing (HPC) cloud infrastructure and the performance prediction recomputed adopting a variation of the CAE model shaped like the actual manufactured part. The process is demonstrated adopting a specific example: the structural assessment of a simplified turbine blade geometry. The baseline geometry, available as a CAD model, is adopted to define the reference FEA model for the ANSYS® Mechanical™ solver so that key performance indexes can be computed (stress level and stiffness). The actual manufactured shape is surveyed and available as a tesselated surface (the standard STL format is herein adopted). The projection and adaption using mesh morphing allows to morph the baseline FEA model onto the actual manufactured shape; finally the updated FEA model is run again to extract performance indexes and decide whether the component fulfills the design specifications.

Keywords:
Digital Twin; Mesh Morphing; FEM; Radial Basis Functions; "As built" design

* Corresponding author. Tel.: +39 0672597124.
E-mail address: biancolini@ing.uniroma2.it

10.1016/j.prostr.2020.02.069

1. Introduction

The technological evolution of many sectors of engineering related to industrial production leads to an increase in the product quality offered, with a reduction in waste and defects thanks to deep efforts in tolerance reduction. The computer-aided engineering (CAE) techniques are now considered as an integral part of mechanical systems design and optimisation process, whenever is required the introduction of robust methodologies able to prevent any critical issues and validate the component in question. The realisation of mechanical systems cannot ignore a verification of the geometric conformity of the real components with nominal models produced by computer-aided design (CAD) tools. Measurement techniques such as blue light scans, photogrammetry and contact-based measurement systems are used to verify the deviation of the real product from the ideal geometry offered by CAD.

The possibility of a digital geometric reconstruction is crucial when it concerns large components, which are subjected to significant changes in geometry as a result of flexibility. In the aeronautical context, for instance, to weaken stresses at points where an aircraft maintenance operation has to be performed, force assignment to jacking positions is addressed in Mongeau and Bes (2005) where a mixed-integer linear programming model is described. A general procedure, based on the fact that geodesic distances are preserved during isometric deformation, is presented in Radvar-Esfahlan and Tahan (2012) to eliminate the use of inspection fixtures. An evolution of the concept is presented in Abenhaim et al. (2015) where a virtual fixture method that predicts the fixed shape of the part is defined by embedding information retrieved from a finite element analysis (FEA) of the nominal CAD model into a boundary displacement constrained optimisation. A compensation technique to face this issue, based on the use of radial basis functions (RBF) mesh morphing and auxiliary CAE model, is presented in Biancolini (2017a): surveyed points are moved onto the undeformed position applying the inverse deformation field computed using FEA modelling and then compared with the baseline geometry to evaluate the shape error. The effect of shape deviation of the manufactured component versus the desired design intent can be evaluated in advance with CAE tools as demonstrated by Kemmler et al. (2014). The shape parameters that are critical for the assembly are, in this case, introduced in the CAE representation as user-controlled shape parameters. The parametric CAE model is thus explored to evaluate with the numerical model how the variations of input parameters are propagated to the system performances.

The described methodology is particularly effective if there is the manufacturer's capability to guarantee that the process tolerances remain below a certain threshold, thus allowing to obtain acceptable performances even in the worst conditions. A statistical approach of this type is typical of large batches production, in which the dimensional control is carried out on a sampled individuals. However, this procedure is not suitable for critical systems, where each part requires a specific control throughout its useful life. In this case the concept of digital twin of the system or component can be pursued (MacDonald et al. (2017)). The digital twin can be synchronised over the time, updating it to the current dimensional state of each individual part and taking into account the original geometry. In this way it is possible to evaluate not only the geometric deviation as a result of the manufacturing phase, but also any variations in the operating phase with the aim of monitoring the trend of the mechanical performance over the time.

On the basis of what described above, metrological techniques are to be considered as a fundamental tool for the geometric verification used to quantify the dimensional deviations from the nominal characteristics. This approach may also involve subsequent interventions with respect to the production of the component such as, for example, checks of faults or modifications that require a new validation of the system. The generation of a digital model as a result of the measurement of the real part allows a considerable saving in terms of time, when compared to the generation of a new CAD model.

The classical approach used to solve the problem of updating the geometry involves the generation of a new CAD model with subsequent CAE modelling and updates to the numerical analysis, as an alternative it is possible to modify the numerical analysis domain, adapting the nominal geometry to the measured one and evaluating the new results obtained. The feasibility of adapt onto "as built" shape in the aeronautical field has been recently demonstrated in Biancolini and Cella (2019) where the transformation of the CAE model of the RIBES wing onto the actual manufactured shape was demonstrated comparing a CAD reconstruction based work flow with an innovative approach based on mesh morphing. An accurate representation of manufactured shapes is specifically felt in aeronautical applications,

as the ones tackled within the RIBES project[1] (Biancolini and Cella (2019)) and RBF4AERO projects[2] that have the objective to improve aircraft performances by means of high fidelity fluid-structure interaction (FSI) numerical analyses (Biancolini et al. (2018b), Papoutsis-Kiachagias et al. (2015), Papoutsis-Kiachagias et al. (2016), Groth et al. (2019), Di Domenico et al. (2018), Biancolini et al. (2016), Andrejašič et al. (2016), Biancolini et al. (2018a)).

Such an innovative strategy based on the adoption of mesh morphing technique founded on RBF (Biancolini et al. (2018b)), is explained in full in the present paper showing how it fits the technical activities of the Experiment n. 12 of Cloudifacturing "Update of CAE models on actual manufactured shapes" (CAE^{Up}) [3]. The paper is comprised of the following sections: after the "Introduction", the description of the workflow and main features of the tool are described in the "CAE^{Up} Experiment" section. Successively in the "CAE Updating Strategies" section the mesh adaption based on the use of RBF, the background of their mathematical framework as well as their use to perform surface projection are respectively reported. Then the practical case of a simplified turbine blade adaption is described in "CAE^{Up} Experiment Application" section. Finally the "Conclusions" section ends the paper.

2. CAE^{Up} Experiment

As already introduced, in modern design processes and methodologies the capability to use the actual geometry of a component for performing CAE calculations acquires paramount importance. Such an objective can be gained adopting the digital twin approach: the CAE model of the system to be analysed is adapted onto the actual manufactured shape thus making the numerical prediction component specific.

Enhancing the previously cited numerical solution proposed in the aeronautical sector to update the numerical CAE models in the respect of the actual manufactured parts (Biancolini and Cella (2019)), a consortium composed of two independent software vendors (RBF Morph s.r.l. and ANSYS Inc.), one value-added reseller (RINA Consulting S.p.A.) and one end user (CMS S.p.A.) submitted a proposal to respond to a Cloudifacturing project call. This proposal succeeded becoming the aforementioned Experiment n.12 named CAE^{Up}.

The mission of Cloudifacturing is to optimise production processes and producibility using high performance computing (HPC) cloud-based modelling and simulation. By leveraging online factory data and advanced data analytic, the project contributes to the competitiveness and resource efficiency of manufacturing SMEs, ultimately fostering the vision of Factories 4.0 and the circular economy. In this context, the CAE^{Up} application aims at implementing a cloudified numerical means capable to rapidly project the nominal CAE model shape onto the digitalised representation of the real component through a mesh morphing technique based on the use of RBF.

In such a way, the performance of the part can be recomputed adopting a variation of the nominal CAE model shaped like the actual manufactured part in view of gaining more accurate and reliable computational outputs and, furthermore, to qualify by calculation even non compliant parts with a clear benefit in terms of production costs.

The rationale of the envisaged process for performing the CAE model updating is shown in Figure 1.

The FEM model of the designed configuration is realised and analysed by means of a FEA software to determine the sought performance indexes. The manufactured part (an automotive tank in the Experiment and a simplified turbine blade in this paper) shape is acquired by means of 3D scan device. These steps are performed on user's infrastructure, i.e. the local workstation on which the user usually performs FEA workflows and the 3D scanning devices usually used for manufactured part inspection. Both FEM model (or alternatively the mesh only) and acquired shape are then transferred to the cloudified application, and the surfaces of the numerical model are updated according to the manufactured shape by means of the projection of the surface mesh nodes onto the acquired shape. If the FEM model is constituted by solid elements, mesh morphing of the whole model is performed in order to uniform the model nodes according to acquired geometry. This step is performed on Cloudifacturing platform. The updated FEM model is finally transferred to users infrastructure and the performance indexes are evaluated on the updated FEM mesh to quantify the impact of shape modifications introduced by the manufacturing process. This step is performed on user's infrastructure.

[1] www.ribes-project.eu.
[2] www.rbf4aero.eu.
[3] https://www.cloudifacturing.eu/exp-12-update-of-cae-models-on-actual-manufactured-shapes/.

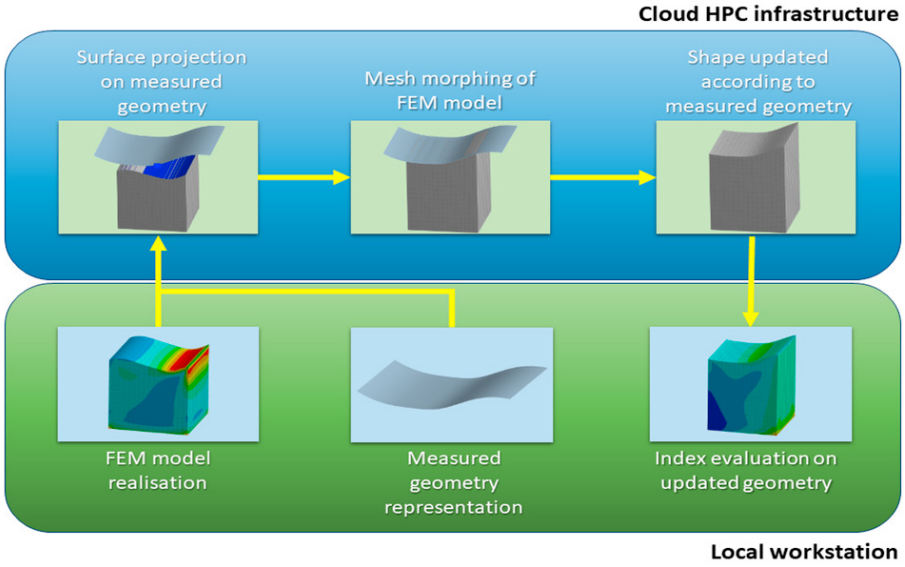

Fig. 1. Process of procedure which the CAE^{Up} application is based on

Considering the process just described, a specific work flow for the usage of CAE^{Up} was designed and it is shown in Figure 2. The main assumptions for the CAE^{Up} usage are that three files need to be provided by the user: the CAE case (ANSYS® Mechanical™ cdb file for the Experiment), the STereo Lithography interface format (STL) file (ASCII) identifying the boundaries of the CAE case and the STL file (ASCII) of the digitalisation (3D scanning) of the manufactured component analysed. Files are required to be aligned correctly, namely same position with respect to the general coordinate system, and generated in the same units.

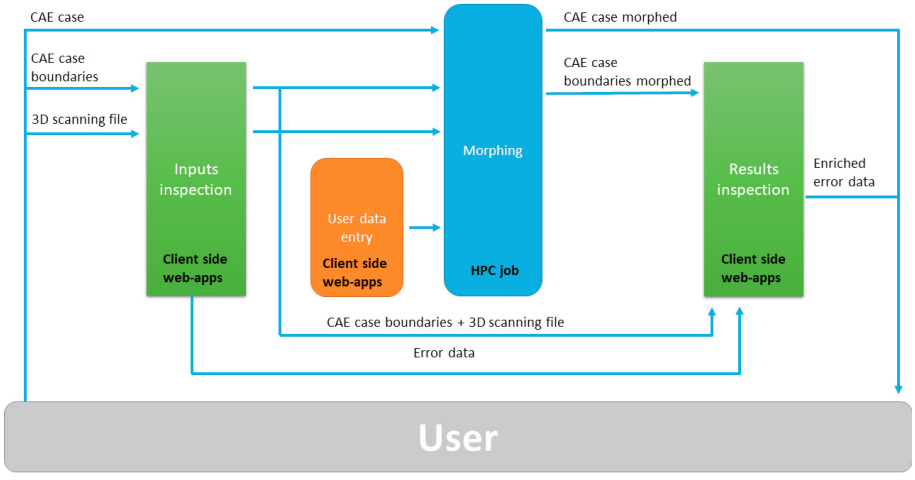

Fig. 2. Workflow of CAE^{Up} functioning

In the first stage of the procedure the user, after logging in on the cloud platform, is required to upload the aforelisted files for running the CAE^{Up} application. Once uploaded, the error data (distributions and histograms) are calculated by processing both the CAE case boundaries file and the 3D scanning file. The error distribution information, generated running the morphing libraries, is envisaged to be provided according to different approaches related to the

mesh morphing projection algorithm. In the ”Inputs inspection” stage the visualisation service is used by the user to visualise CAE case boundaries and 3D scanning files, as well as error maps and histograms.

Successively the user is asked to insert some inputs dealing with the mesh morphing projection algorithm and solver settings. Once these data are entered, the user launches morphing libraries which update the CAE case. In this stage, the morphing solution is also used to update the file of CAE boundaries for visualisation purpose. When the ”Morphing” stage is finished, in the ”Results inspection” stage the user is allowed to visualise the morphed configuration of the CAE case boundaries as well. The error maps and histograms are enriched accordingly. At the end of the process, the user can download the files of interest on a local machine.

The requirements dealing with the update accuracy performed on complex geometry and the minimum interaction requested to the user, pose a challenging objective related to the development of high demanding mesh morphing functionality. As such, an effective and robust mathematical framework for surface mesh nodes projection and volume smoothing need to be implemented (see section 3).

It is worth to mention that, thanks to the mesh-less characteristic of the RBF mesh morphing, the CAE^{Up} approach turns out to be solver agnostic, meaning that it can be applied to any type of CAE model providing that its mesh nodes coordinates can be modified.

3. CAE Updating Strategies

The process to update the CAE model onto the manufactured shape usually receives, as input, the baseline CAE model (the computational mesh for CFD analysis and/or the one for FEA analyses) and the actual geometry of the surveyed manufactured component (that we suppose to be available as a tessellated surface which has been already filtered and processed to be representative of the shape). Desired output is a variation of the CAE model onto the manufactured shape.

As already introduced, a mesh morphing approach is adopted in this study. It allows to update the CAE by the adaptation of the existing computational domain onto the new tessellated surface, without the burden of creating a new CAD model and its grid. In this process the mesh topology is preserved with further advantages in term of computational robustness and consistency.

3.1. Mesh adaption based on radial basis functions

Radial basis functions (RBF) are considered one of the most effective algorithms in solving problems related to mesh morphing (Jakobsson and Amoignon (2007)). One of the major advantages of this type of approach is its *mesh less* nature, which allows the RBF approach to support every type of topology and discretisation. The RBF method can be used, as anticipated, also starting from STL type surfaces, this eventually allows to filter also any noise present inside point clouds inserted as input. An aspect that can be considered as critical of the RBF is related to the high computational cost required for the execution of the algorithm, since this requires a number of equations equal to the number of source points involved. However the solving process can be accelerated thanks to the parallelisation and implementation of specific optimisation algorithms (Rendall and Allen (2009)).

RBF mesh morphing (de Boer et al. (2007)) of computational mesh is a common practice for shape optimisation and multi-physics analyses. RBF Morph™ software[4] offers several examples of industrial applications of RBF mesh morphing. Initially developed as an Add On for the CFD solver ANSYS Fluent (Biancolini (2012)), the method was then adapted to FEA models such as an ACT Extension for Mechanical (Cenni et al. (2016), Porziani et al. (2018),Biancolini et al. (2018c), Giorgetti et al. (2018)). The tool allows a mesh morphing workflow approach similar to the one described in Sieger et al. (2014), with a strong interaction between the meshed domain and the underlying CAD geometry. In Cella and Biancolini (2012), a relevant example of fluid structure interaction (FSI) analyses supported by RBF Mesh morphing is given, where the CFD mesh of a complete aircraft is updated according to FEA solutions. Within the RBF4AERO EU FP7 project[5] an intensive application of FSI has been tested. Since RBFs method results to be mesh less, it can be considered free from interactive sculpting tools (Botsch and Kobbelt (2005))

[4] www.rbf-morph.com.
[5] www.rbf4aero.eu.

and particularly effective for real time editing: in Valentini and Biancolini (2018) it is present an integration based on augmented reality and a haptic device. An example of shape optimisation, in which each explored design point is fully computed using the FSI approach, is given in Andrejašič et al. (2016).

3.2. RBF Theory Background

Radial basis functions were firstly introduced as an interpolation method for scattered data by Hardy (1990). They provide a tool to interpolate everywhere in the space a scalar function defined at discrete points giving the exact values at original points. The RBF equation is represented as:

$$s(\mathbf{x}) = \sum_{i=1}^{N} \gamma_i \varphi \left(\| \mathbf{x} - \mathbf{x}_{s_i} \| \right) + h(\mathbf{x}) \tag{1}$$

The scalar function $s(.)$ is defined for an arbitrary sized variable $\mathbf{x}$ and represents a transformation defined in a multi-dimensional space ($\mathbb{R}^n \longrightarrow \mathbb{R}$). At a given point $\mathbf{x}$ the value of the RBF is obtained accumulating the interactions with all source points $\mathbf{x}_{s_i}$ gained computing the radial distance between $\mathbf{x}$ and each $\mathbf{x}_{s_i}$ processed by the radial interaction function $\varphi(.)$, consisting of a transformation $\mathbb{R} \longrightarrow \mathbb{R}$, which is then multiplied by the weight γ_i that can be seen as the "intensity" of the source point. In some cases, the polynomial term h is added. The summation of the radial contribution of each source point (RBF centre) and of a polynomial term eventually present is capable of express the scalar function at an arbitrary location inside or outside the domain (interpolation/extrapolation), as soon as the unknown coefficients are determined, according to equation 1.

The possibility to interpolate using radial basis functions still holds for scalar fields, but the fit can be repeated many times using the same interpolation and constraint matrixes. In this case, a rectangular matrix takes the place of the g vector, it is then solved on a column wise fashion computing the coefficients γ and β related to each column. If a deformation vector field has to be fitted in 3D (space warping or mesh morphing that in this study is performed using the full supported radial function $\varphi(r) = |r|$), each component of the displacement prescribed at the source points is interpolated as follows

$$\begin{cases} s_x(\mathbf{x}) = \sum_{i=1}^{N} \gamma_i^x \varphi \left(\| \mathbf{x} - \mathbf{x}_{s_i} \| \right) + \beta_0^x + \beta_1^x x + \beta_2^x y + \beta_3^x z \\ s_y(\mathbf{x}) = \sum_{i=1}^{N} \gamma_i^y \varphi \left(\| \mathbf{x} - \mathbf{x}_{s_i} \| \right) + \beta_0^y + \beta_1^y x + \beta_2^y y + \beta_3^y z \\ s_z(\mathbf{x}) = \sum_{i=1}^{N} \gamma_i^z \varphi \left(\| \mathbf{x} - \mathbf{x}_{s_i} \| \right) + \beta_0^z + \beta_1^z x + \beta_2^z y + \beta_3^z z \end{cases} \tag{2}$$

The passage of the interpolated function through all the points of the original dataset is still guaranteed by the RBF fitting process, while the characteristics of the function between points (interpolation) or outside the dataset (extrapolation) depends on the radial function used. The fit process and the evaluation of global supported RBF can be accelerated with methods such as the Fast Multiple Method, which has been demonstrated to be very effective for poly harmonics splines by Beatson et al. (2007). The first applications of RBF regarded interpolation tools for scatter data, we recalla 1971 publication by Rolland Hardy (Editor (1992)) about multi quadric (MQ) RBF for the representation of topographic surveyed locations.

3.3. Use of RBF for Surface Projection

The geometrical information available from metrology techniques are commonly in form of a cloud of points from which automatic triangulation and filtering procedures are used to provide a tessellated surface. The output STL surface is used as target for the morphing action of the CAE mesh.

A cubic spline $\varphi(r) = |r|^3$ is considered in the interpolant formulation expressed by equation 1 which gets the form

$$s(\mathbf{x}) = \sum_{i=1}^{N} \gamma_i \left(\sqrt{(x - x_{s_i})^2 + (y - y_{s_i})^2 + (z - z_{s_i})^2} \right)^3 + h(\mathbf{x}) \tag{3}$$

Taking into account on-surface and off-surface points distribution, the zero iso-surface of the function $s(\mathbf{x})$ is built, this one represents the interpolating implicit surface. Off-surface points are obtained generating two points for each on-surface one, inward and outward along the normal direction at a prescribed distance. Offset distance should be small enough to avoid off-surface points clashes at small radius of curvature regions of the surface. The projection onto the implicit surface is carried out by Newton's iteration method. The gradient of the function $s(\mathbf{x})$ is

$$\nabla s(\mathbf{x}) = \left\{ \frac{\partial s(\mathbf{x})}{\partial x} \quad \frac{\partial s(\mathbf{x})}{\partial y} \quad \frac{\partial s(\mathbf{x})}{\partial z} \right\}^T \tag{4}$$

where

$$\begin{aligned}
\tfrac{\partial s(\mathbf{x})}{\partial x} &= 3 \textstyle\sum_{i=1}^{N} \gamma_i (x - x_{s_i}) \sqrt{(x - x_{s_i})^2 + (y - y_{s_i})^2 + (z - z_{s_i})^2} + \beta_1 \\
\tfrac{\partial s(\mathbf{x})}{\partial y} &= 3 \textstyle\sum_{i=1}^{N} \gamma_i (y - y_{s_i}) \sqrt{(x - x_{s_i})^2 + (y - y_{s_i})^2 + (z - z_{s_i})^2} + \beta_2 \\
\tfrac{\partial s(\mathbf{x})}{\partial z} &= 3 \textstyle\sum_{i=1}^{N} \gamma_i (z - z_{s_i}) \sqrt{(x - x_{s_i})^2 + (y - y_{s_i})^2 + (z - z_{s_i})^2} + \beta_3
\end{aligned} \tag{5}$$

The projection of a point $\mathbf{x}$ onto the implicit surface can then be calculated iteratively by

$$\mathbf{x}_{k+1} = \mathbf{x}_k + \frac{s(\mathbf{x}_k)}{\|\nabla s(\mathbf{x}_k)\|^2} \nabla s(\mathbf{x}_k) \tag{6}$$

The above iteration runs until $\|\mathbf{x}_{k+1} - \mathbf{x}_k\|$ is less than a given tolerance.

Surface projection concept is shown in figure 3 by Biancolini (2017c). The left figure highlights the centroids of the target, which are used for the generation of on-surface and off-surface points. The projection field is used to adapt the mesh of a cube (right figure) to a new shape with a fillet . A work flow based on two or more steps can be used for the projection process in the event that the shape of the target surface is significantly different from the source or is not aligned with the nominal geometry. In these cases, the preliminary step consists in a small local RBF problem in which a set of landmark positions, corresponding to the predefined locations already existing onto the baseline geometry, are identified and used as sources points. This strategy allows to recover rigid motions and global deformations. An example of this work flow is reported in Biancolini and Valentini (2018).

The level of detail and complexity of the surface deeply affects the size of the RBF problem. The strategy adopted to increase the capabilities of the projection procedure implemented in the RBF Morph software, relies on the generation of overlapping sub-domains adopting partition of unity (POU) methods Babuška and Melenk (1998), with the following decomposition into smaller problems. The computational cost of the process grows linearly with the number of centres. The reduction of the number of points in each sub-domain allows to reduce the computation time. The direct fit of the RBF using a linear solver is accelerated by a fast iterative solver in which the cost of a single iteration consists of a self-evaluation of the RBF at all centres Biancolini (2017b). The cost is, however, almost proportional to the square of the number of RBF centres. The adoption of POU allows to reduce hours in minutes.

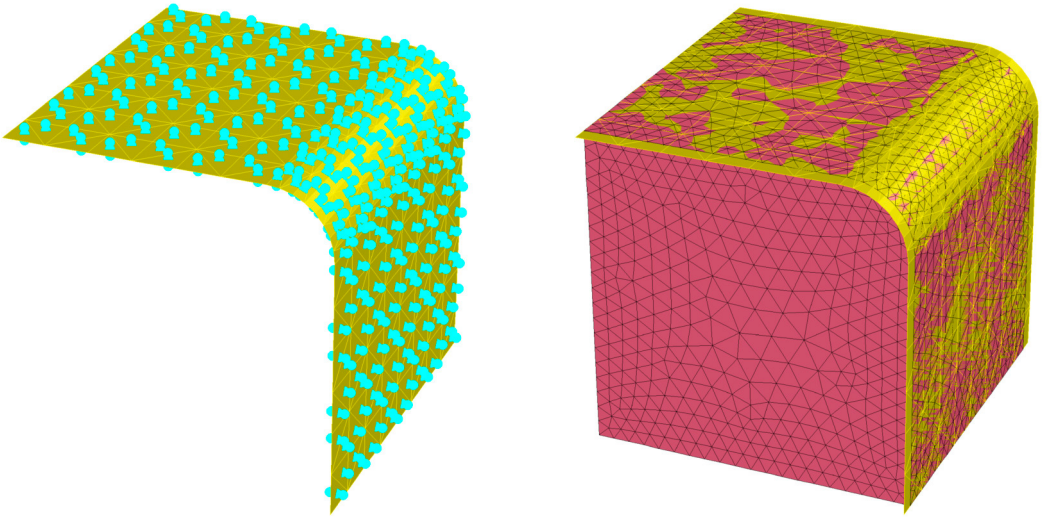

Fig. 3. The implicit surface (left) allows to add a fillet onto the sharp edge of a cube (right) by RBF mesh morphing (Biancolini (2017b))

4. CAE^{Up} Experiment Application

As already introduced the example described in this paper examines the effects of manufacturing errors on a simplified turbine blade model. All operations concerning the study were carried out using commercial software working in the ANSYS Workbench platform: ANSYS SpaceClaim, ANSYS Meshing, ANSYS Mechanical and RBF Morph developed through the ANSYS ACT technology.

Such simplified mock-up geometry was selected to be representative enough to demonstrate the concept. However the actual manufacture is not available and so the ”actual” 3d scanned shape to be used as a target was generated by perturbing the baseline one. The biological growth method (BGM) approach adopted in Porziani et al. (2018) was exploited to generate such artificial shape. In particular, the BGM technique utilised, foresees two steps: in the first one a stress field was created by applying a variable pressure field on the pressure side fillet as shown in Figure 4, and by fixing both the tip and root of the blade.

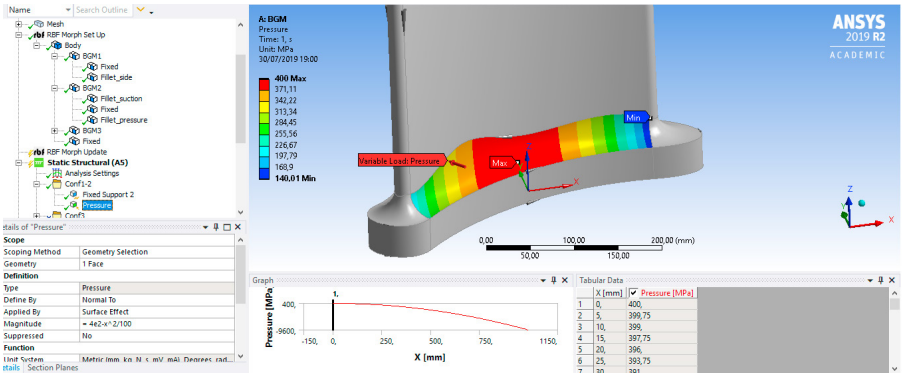

Fig. 4. Fictional pressure field applied to the blade fillet for BGM distortion

Regarding the mesh set-up, tetrahedral elements were chosen for the entire body to better simulate the tessellated scan geometry and, furthermore, to fit the need for simplify the reconstruction of the solid geometry from it; in particular, a Face Meshing control was adopted to obtain regular faceted surfaces. The element size was set to 4mm, that

represents a compromise between surface precision and computational time for morphing. As a result, the Mechanical Model presented 478620 nodes and 278362 elements. With this configuration, the maximum equivalent stress, evaluated according to von Mises, reached about 800 MPa in the central area of the pressure side fillet, while in the lateral side of the fillet it was measured the minimum, nearly 0 MPa.

In the second stage, the resulting equivalent stress field, evaluated according to von Mises, was then imposed as starting point of the process in which mesh morphing is driven by stresses and a user-defined threshold value. In the morphing solution set-up, the chosen maximum offset of the fillet surfaces was 0.4mm, because it was judged to be reasonably close to the maximum manufacturing tolerance for blade characterised by a chord length of 345 mm.

Considering the above mentioned stress values, in RBF Morph Set Up three different first level child objects were created: the first one acting on the leading edge and trailing edge fillet, with a Threshold value of 25 MPa; the second one, with further two second level child objects, acting on the pressure side fillet and the suction side fillet, respectively with a Threshold value of 600 MPa and 500 MPa; the last one acting on the airfoil with a Threshold value set to 4 MPa. Doing so, the process resulted in a morphed configuration that reduced the thickness of the airfoil at the fillet and, consequently, increased the stress caused by the assigned loading configuration.

Exporting the mesh of the morphed model in STL format the fictitious 3D scanning file was finally obtained. The distribution of the geometrical deviation between the nominal CAE model mesh and the fictitious 3D scanning file is depicted in Figure 5 from a frontal and rear perspective. As visible, the largest differences are in the fillet area, and the maximum deviation values are 0.38 mm for the inside area and 0.28 mm for the outside area.

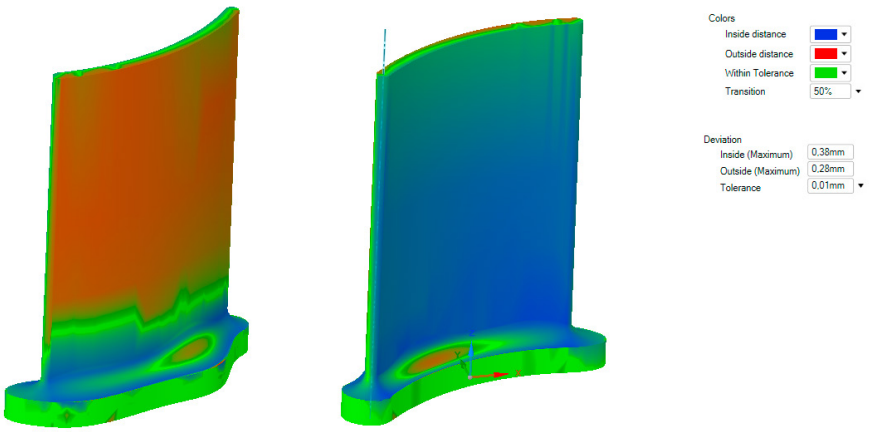

Fig. 5. Colour map of the deviation between ideal and manufactured geometries

Once both the source and target geometries are defined, the two models are imported in a Workbench project. Even for the stress analysis, to fit the conformation of the blade a tetrahedral mesh is adopted for the source body, while the target body is treated as Construction Body; to appreciate the differences between original and manufactured, a high level of refinement is needed resulting in 479525 nodes and 279069 elements.

Then, with the RBF Morph extension, each source surface is projected on the corresponding target creating a first level child object, while the related edges are projected using second level child elements.

The resulting mesh matches almost perfectly the target model: as visible in Figure 6, the distance of almost all the sample points of the morphed body form the target one is less than 0.01mm, while some areas at the fillet result slightly deviated from the target; anyway, the measured difference between the two geometries is contained within an interval of 0.03mm, that means less than 8% of the manufacturing tolerance. However, it can be noted that, near the root edges, the detected peak is considerable high respect to the tolerance itself: to reduce the computational cost, these edges were indeed not projected on the target, considering that the stress analysis would not have been significantly influenced.

To test the goodness of the mesh morphing process, it was also made a comparison between element quality of the original mesh and the morphed mesh. As shown in Figure 8, the shape of the distribution is quite similar, even if a little amount of high quality elements (about 5600, that is 2% of the entire mesh) is declassed after the morphing. In

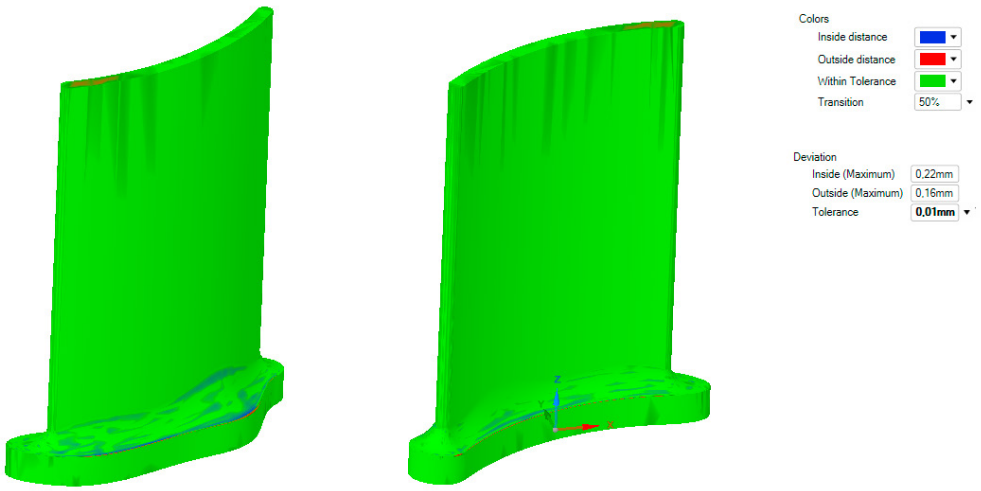

Fig. 6. Colour map of the deviation between morphed geometry and target geometry

particular, the average quality decreases from 0.69 to 0.68, that corresponds to a reduction of less than 1.5% of the initial value. Thus, the loss of quality can be considered negligible for the examined case

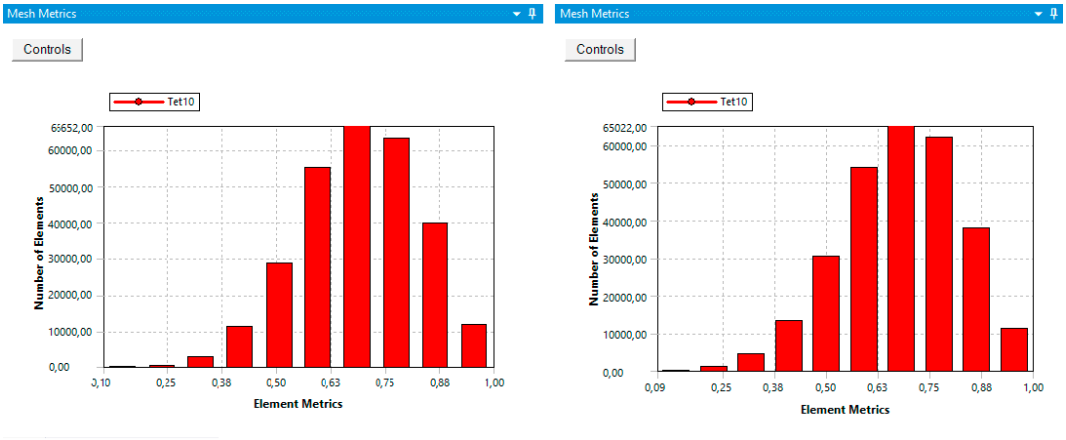

Fig. 7. Element Quality before and after mesh morphing

Assuming the material to be isotropic, linear and elastic, the static structural analysis on the morphed and original geometry was performed by means of ANSYS Mechanical. The computed equivalent von Mises stress distribution for the morphed model and the original geometry is shown in Figure 8 respectively on the left and right side.

The numerical solution shows a little increase of the maximum equivalent stress that changes from 109 MPa to 111 MPa approximately, namely below 2% in absolute terms. This means that errors within 0.4 mm of tolerance affects only a bit the stresses.

5. Conclusions

The problem of the geometric reconstruction of virtual objects derived from optical or contact based metrology techniques is a relevant topic when verifying manufactured products. Moreover, it is particularly felt in the creation of digital twins as well as in the verification of design modification requirements.

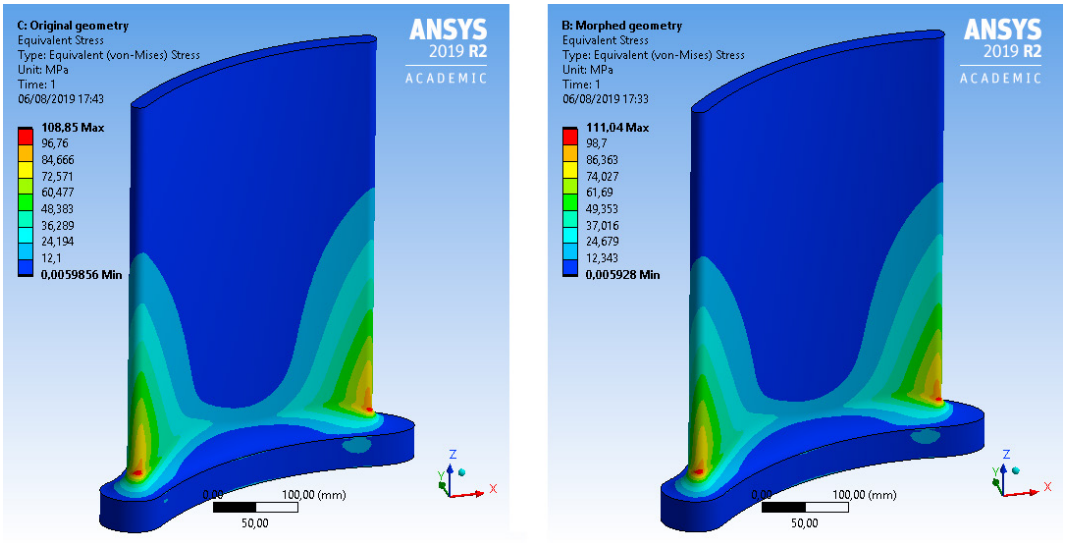

Fig. 8. Stress comparison between morphed geometry and original geometry

In this paper a solver independent numerical procedure to adapt CAE models onto the actual manufactured shape of systems to be simulated so to generate the digital twin of the real product as built, was described. The use of such procedure, based on the use of RBF mesh morphing, was showcased using a test case consisting of a simplified version of a turbine blade calculating the difference between the stress field of the baseline nominal configuration and of the morphed one reproducing the manufactured component.

The development of the study demonstrated the effectiveness of the proposed procedure as well as the high accuracy of the projection applied through RBF mesh morphing. The error between the peak equivalent stress of the baseline and morphed configuration was found to be very limited.

Adopting such an approach, a numerical means will be developed and made available on the cloud to offer CAE services through the Cloudifacturing marketplace according to the software as a service (SaaS) paradigm. Such a cloudified application will enable users to verify the actual geometry after manufacturing, or repairing, and to also qualify through CAE tools and simulations even non compliant parts with a consequent decrease of production costs.

The most important conclusion of the presented work is that surface projecting technique based on the use of RBF mesh morphing confirmed to guarantee high accuracy and flexibility in tackling geometrical reconstruction problems providing the capability to significantly reduce the effort if compared to a model reconstruction procedure adopting CAD systems.

6. Acknowledgements

Authors want to thank the project Cloudifacturing which receives funding from the European Unions Horizon 2020 research and innovation programme under Grant Agreement no. 768892.

References

Abenhaim, G.N., Desrochers, A., Tahan, A.S., Bigeon, J., 2015. A virtual fixture using a FE-based transformation model embedded into a constrained optimization for the dimensional inspection of nonrigid parts. Computer-Aided Design 62, 248 – 258. URL: http://www.sciencedirect.com/science/article/pii/S0010448514002899, doi:https://doi.org/10.1016/j.cad.2014.12.006.

Andrejašič, M., Eržen, D., Costa, E., Porziani, S., Biancolini, M., Groth, C., 2016. A mesh morphing based FSI method used in aeronautical optimization applications, in: ECCOMAS Congress 2016 - Proceedings of the 7th European Congress on Computational Methods in Applied Sciences and Engineering.

Babuška, I., Melenk, J.M., 1998. The Partition of Unity method. International Journal for Numerical Methods in Engineering 40, 727 – 758. doi:10.1002/(SICI)1097-0207(19970228)40:4<727::AID-NME86>3.0.CO;2-N.

Beatson, R.K., Powell, M.J.D., Tan, A.M., 2007. Fast evaluation of polyharmonic splines in three dimensions. IMA Journal of Numerical Analysis 27, 427–450. URL: http://dx.doi.org/10.1093/imanum/drl027, doi:10.1093/imanum/drl027.

Biancolini, M., Cella, U., Groth, C., Genta, M., 2016. Static Aeroelastic Analysis of an Aircraft Wind-Tunnel Model by Means of Modal RBF Mesh Updating. Journal of Aerospace Engineering 29. doi:10.1061/(ASCE)AS.1943-5525.0000627.

Biancolini, M., Chiappa, A., Giorgetti, F., Groth, C., Cella, U., Salvini, P., 2018a. A balanced load mapping method based on radial basis functions and fuzzy sets. International Journal for Numerical Methods in Engineering 115, 1411–1429.

Biancolini, M., Chiappa, A., Giorgetti, F., Groth, C., Cella, U., Salvini, P., 2018b. A balanced load mapping method based on Radial Basis Functions and fuzzy sets. International Journal for Numerical Methods in Engineering 115, 1411 – 1429. URL: https://onlinelibrary.wiley.com/doi/abs/10.1002/nme.5850, doi:10.1002/nme.5850, arXiv:https://onlinelibrary.wiley.com/doi/pdf/10.1002/nme.5850.

Biancolini, M., Chiappa, A., Giorgetti, F., Porziani, S., Rochette, M., 2018c. Radial basis functions mesh morphing for the analysis of cracks propagation. Procedia Structural Integrity 8, 433–443.

Biancolini, M.E., 2012. Mesh morphing and smoothing by means of Radial Basis Functions (RBF): A practical example using fluent and rbf morph, in: Leng, J., Sharrock, W. (Eds.), Handbook of Research on Computational Science and Engineering: Theory and Practice.

Biancolini, M.E., 2017a. Compensation of metrological data, in: Fast Radial Basis Functions for Engineering Applications. chapter 12.6, pp. 313 – 319.

Biancolini, M.E., 2017b. Iterative solvers, in: Fast Radial Basis Functions for Engineering Applications. chapter 3.7, pp. 58 – 59.

Biancolini, M.E., 2017c. RBF implicit representation of geometrical entities, in: Fast Radial Basis Functions for Engineering Applications. chapter 5, pp. 81 – 92.

Biancolini, M.E., Cella, U., 2019. Radial basis functions update of digital models on actual manufactured shapes. Journal of Computational and Nonlinear Dynamics 14, 021013.

Biancolini, M.E., Valentini, P.P., 2018. Virtual human bone modelling by interactive sculpting, mesh morphing and force-feedback. International Journal on Interactive Design and Manufacturing (IJIDeM) URL: https://doi.org/10.1007/s12008-018-0487-3, doi:10.1007/s12008-018-0487-3.

de Boer, A., van der Schoot, M., Bijl, H., 2007. Mesh deformation based on Radial Basis Functions interpolation. Computers & Structures 85, 784 – 795. URL: http://www.sciencedirect.com/science/article/pii/S0045794907000223, doi:https://doi.org/10.1016/j.compstruc.2007.01.013.

Botsch, M., Kobbelt, L., 2005. Real-time shape editing using Radial Basis Functions. Computer Graphics Forum 24, 611 – 621. URL: https://onlinelibrary.wiley.com/doi/abs/10.1111/j.1467-8659.2005.00886.x, doi:10.1111/j.1467-8659.2005.00886.x, arXiv:https://onlinelibrary.wiley.com/doi/pdf/10.1111/j.1467-8659.2005.00886.x.

Cella, U., Biancolini, M.E., 2012. Aeroelastic analysis of aircraft wind-tunnel model coupling structural and fluid dynamic codes. AIAA Journal of Aircraft 49, 407 – 414. URL: https://doi.org/10.2514/1.C031293, doi:10.2514/1.C031293.

Cenni, R., Bertuzzi, G., Cova, M., 2016. A CAD-MESH mixed approach to enhance shape optimization capabilities, in: CAE Conference, Parma, Italy.

Di Domenico, N., Groth, C., Wade, A., Berg, T., Biancolini, M., 2018. Fluid structure interaction analysis: vortex shedding induced vibrations. Procedia Structural Integrity 8, 422–432. URL: https://doi.org/10.1016/j.prostr.2017.12.042http://linkinghub.elsevier.com/retrieve/pii/S2452321617305358, doi:10.1016/j.prostr.2017.12.042.

Editor, 1992. Biographical sketch of rolland l. hardy. Computers Math Applic. 24, ix – x.

Giorgetti, F., Cenni, R., Chiappa, A., Cova, M., Groth, C., Pompa, E., Porziani, S., Biancolini, M.E., 2018. Crack propagation analysis of near-surface defects with radial basis functions mesh morphing. Procedia Structural Integrity 12, 471–478.

Groth, C., Cella, U., Costa, E., Biancolini, M., 2019. Fast high fidelity cfd/csm fluid structure interaction using rbf mesh morphing and modal superposition method. Aircraft Engineering and Aerospace Technology URL: https://www.scopus.com/inward/record.uri?eid=2-s2.0-85064015261&doi=10.1108%2fAEAT-09-2018-0246&partnerID=40&md5=4c6e2f39a42059f64b9b8f5b99dc0175, doi:10.1108/AEAT-09-2018-0246. cited By 0.

Hardy, R., 1990. Theory and applications of the multiquadric-biharmonic method 20 years of discovery 19681988. Computers & Mathematics with Applications 19, 163 – 208. URL: http://www.sciencedirect.com/science/article/pii/089812219090272L, doi:https://doi.org/10.1016/0898-1221(90)90272-L.

Jakobsson, S., Amoignon, O., 2007. Mesh deformation using Radial Basis Functions for gradient-based aerodynamic shape optimization. Computers & Fluids 36, 1119 – 1136. URL: http://www.sciencedirect.com/science/article/pii/S0045793006001320, doi:https://doi.org/10.1016/j.compfluid.2006.11.002.

Kemmler, S., Dazer, M., Leopold, T., Bertsche, B., 2014. Method for the development of a functional adaptive simulation model for designing robust products, in: Weimar Optimization and Stochastic Days.

MacDonald, C., Dion, B., Davoudabadi, M., 2017. Creating a digital twin for a pump. ANSYS Advantage 1, 8 – 10.

Mongeau, M., Bes, C., 2005. Aircraft maintenance jacking problem via optimization. IEEE Transactions on Aerospace and Electronic Systems 41, 99 – 109. doi:10.1109/TAES.2005.1413750.

Papoutsis-Kiachagias, E., Andrejasic, M., Porziani, S., Groth, C., Erzen, D., Biancolini, M., Costa, E., Giannakoglou, K., 2016. Combining an RBF-based morpher with continuous adjoint for low-speed aeronautical optimization applications, in: ECCOMAS Congress 2016 - Proceedings of the 7th European Congress on Computational Methods in Applied Sciences and Engineering.

Papoutsis-Kiachagias, E.M., Porziani, S., Groth, C., Biancolini, M.E., Costa, E., Giannakoglou, K.C., 2015. Aerodynamic Optimization of Car Shapes using the Continuous Adjoint Method and an RBF Morpher. EUROGEN 2015, 11th International Conference on Evolutionary and Deterministic Methods for Design, Optimization and Control with Applications to Industrial and Societal Problems , 1–15doi:10.13140/RG.2.1.1615.2165.

Porziani, S., Groth, C., Biancolini, M.E., 2018. Automatic shape optimization of structural components with manufacturing constraints. Procedia

Structural Integrity 12, 416–428.

Radvar-Esfahlan, H., Tahan, S.A., 2012. Nonrigid geometric metrology using generalized numerical inspection fixtures. Precision Engineering 36, 1 – 9. URL: http://www.sciencedirect.com/science/article/pii/S0141635911000997, doi:https://doi.org/10.1016/j.precisioneng.2011.07.002.

Rendall, T., Allen, C., 2009. Efficient mesh motion using Radial Basis Functions with data reduction algorithms. Journal of Computational Physics 228, 6231 – 6249. URL: http://www.sciencedirect.com/science/article/pii/S0021999109002721, doi:https://doi.org/10.1016/j.jcp.2009.05.013.

Sieger, D., Menzel, S., Botsch, M., 2014. RBF morphing techniques for simulation-based design optimization. Eng. Comput. (Lond.) 30, 161–174. URL: https://doi.org/10.1007/s00366-013-0330-1, doi:10.1007/s00366-013-0330-1.

Valentini, P.P., Biancolini, M.E., 2018. Interactive sculpting using augmented-reality, mesh morphing, and force feedback: Force-feedback capabilities in an augmented reality environment. IEEE Consumer Electronics Magazine 7, 83–90. doi:10.1109/MCE.2017.2709598.